



## Early View

Original article

### **Cross-reactive antibodies against dust mite-derived enolase induce neutrophilic airway inflammation**

Jianli Lin, Nana Huang, Jing Li, Xiaoyu Liu, Qing Xiong, Chengshen Hu, Desheng Chen, Lvxin Guan, Kexin Chang, Dang Li, Stephen Kwok-Wing Tsui, Nanshan Zhong, Zhigang Liu, Ping-Chang Yang

Please cite this article as: Lin J, Huang N, Li J, *et al.* Cross-reactive antibodies against dust mite-derived enolase induce neutrophilic airway inflammation. *Eur Respir J* 2020; in press (<https://doi.org/10.1183/13993003.02375-2019>).

This manuscript has recently been accepted for publication in the *European Respiratory Journal*. It is published here in its accepted form prior to copyediting and typesetting by our production team. After these production processes are complete and the authors have approved the resulting proofs, the article will move to the latest issue of the ERJ online.

## **Cross-reactive antibodies against dust mite-derived enolase induce neutrophilic airway inflammation**

**Running title:** HDM-derived enolase induces airway neutrophilic inflammation

Jianli Lin<sup>1, 2#</sup>, Nana Huang<sup>1#</sup>, Jing Li<sup>2#</sup>, Xiaoyu Liu<sup>1#</sup>, Qing Xiong<sup>3</sup>, Chengshen Hu<sup>1</sup>, Desheng Chen<sup>1</sup>, Lvxin Guan<sup>1</sup>, Kexin Chang<sup>1</sup>, Dang Li<sup>1</sup>, Stephen Kwok-Wing Tsui<sup>3</sup>, Nanshan Zhong<sup>2\*</sup>, Zhigang Liu<sup>1\*</sup>, Ping-Chang Yang<sup>1,4\*</sup>

1. State Key Laboratory of Respiratory Disease for Allergy at Shenzhen University; Shenzhen University School of Medicine, Shenzhen, China.

2. State Key Laboratory of Respiratory Disease, National Clinical Center for Respiratory Diseases, Guangzhou Institute of Respiratory Diseases, First Affiliated Hospital, Guangzhou Medical University, Guangzhou, China.

3. School of Biomedical Sciences, Chinese University of Hong Kong, Hong Kong, China.

4. Guangdong Provincial Key Laboratory of Regional Immunity and Diseases, Shenzhen, China.

#These authors equally contributed to this work

**\*Corresponding authors:** Dr. Ping-Chang Yang ([pcy2356@szu.edu.cn](mailto:pcy2356@szu.edu.cn)), Dr. Zhigang Liu

([lzg@szu.edu.cn](mailto:lzg@szu.edu.cn)) and Dr. Nanshan Zhong ([nanshan@vip.163.com](mailto:nanshan@vip.163.com) Room).

Room A7-509 at Lihu Campus, Shenzhen University School of Medicine. 1066 Xueyuan Blvd, Shenzhen 518055, China. Tel:

8675586172722. Fax: 8675586671906.

## **Abstract**

**Background and aims:** Neutrophilic inflammation is a hallmark of some specific asthma phenotypes; its etiology is not fully understood yet. House dust mite (HDM) is the most common factor involving with the pathogenesis of airway inflammation. This study aims to elucidate the role of cross-antibodies against HDM-derived factors in the development of neutrophilic inflammation in the airway.

**Methods:** Blood samples were collected from asthma patients with chronic neutrophilic asthma to be analyzed the HDM-specific cross-reactive antibodies. The role of an antibody against HDM-derived enolase (EnoAb) in the impairment of airway epithelial barrier function and induction of airway inflammation was assessed in a cell culture model and an animal model.

**Results:** High similarity (72%) of the enolase gene sequences was identified between HDM and human. Serum EnoAb was detected in patients with chronic neutrophilic asthma. The EnoAb bound to airway epithelial cells to form complexes with enolase, which activated complements, impaired airway epithelial barrier functions and induced neutrophilic inflammation in the airway tissues.

**Conclusions:** HDM-derived enolase can induce specific cross-antibodies by human, which induce neutrophilic inflammation in the airway.

**Keywords:** House dust mite; asthma; epithelial barrier; cross-antibody; inflammation.

## Introduction

Airway chronic inflammation generally features as profound inflammatory cell infiltration in the airway mucosa [1]. The inflammatory activities result in narrow airway calibration and make patients difficulty to breath [2]. The causative factors of chronic airway inflammation are various. Allergic responses are one of the major causes, in which house dust mite (HDM)-derived allergens are the canonical factors to contribute to the pathogenesis of allergic responses in the airway mucosa [3]. Although research in airway allergic inflammation advances rapidly in the last a few decades, the initiating factors of airway chronic inflammation and the underlying mechanism remain to be further investigated [4]. The therapeutic effects of airway inflammation are not satisfactory currently [5]. Thus, it is necessary to further investigate the mechanism and invent novel and effective therapies for chronic airway inflammation.

The airway epithelium is an interface between the body and external environment. Some allergens, such as those derived from HDM, can be absorbed by epithelial cells. Although there is an enzyme system in epithelial cells that can degrade the absorbed protein antigens into small peptides or amino acids, some peptides with competent antigenicity may be transported to the subepithelial regions where the antigens contact immune cells and initiate immune responses [6]. The immune cells thereby produce antigen-specific immunoglobulin (Ig)E or/and antigen-specific IgG. IgE binds to the high affinity receptors on mast cells to make mast cells sensitized. Re-exposure to specific antigen activates sensitized mast cells. The mast cells release chemical mediators to evoke allergic responses [7]. On the other hand, the specific IgG can bind specific antigens to form complexes. The complexes may be cleaned by phagocytes, or activate the complement system to chemoattract neutrophils and induce inflammation in the local tissues [8, 9]. Yet, whether such complexes

associate with the pathogenesis of airway chronic inflammation has not been defined.

It is recognized that the gene sequences of some extrinsic proteins, such as airborne allergens may be the same as that of some proteins in the human body. After getting into the body, the immune system may produce antibodies against the extrinsic proteins [10]. Apart from recognizing the specific extrinsic proteins, the antibodies may also recognize proteins in the human body with similar gene sequences to the extrinsic proteins [11]. These antibodies are designated cross-antibodies. Homologous antibodies have cross reactivity; such as those against streptococcal-vimentin induce microvascular cardiac endothelial proinflammatory phenotype in rheumatic heart disease [12]. The cross-antibodies may form complexes with specific constitutive homologous antigens. The complexes activate complement system, chemoattract inflammatory cells and induce inflammation on the site [13]. Previous studies indicate that enolase-specific antibodies are associated with the pathogenesis of mucosal inflammation, e.g., inflammatory bowel disease [14]. Enolase is a metalloenzyme in glycolysis and exists in all tissues and all organisms [15]. Our previous study found that the gene of HDM-derived enolase had high similarity to human enolase [16]. Whether the enolase cross-antibodies are involved in the pathogenesis of airway chronic inflammation remains to be further investigated.

Neutrophilic asthma is a subtype of asthma, which is featured as many neutrophils gather in the lung tissue as well as appear in the airway tract [17]. These neutrophils release inflammatory mediators to induce inflammation in the local tissues [17]. The causative factors of neutrophilic asthma remain largely unknown and need to be further investigated.

As IgG autoantibody-induced cytotoxicity against airway epithelial cells plays a role in the pathogenesis of nonallergic asthma [18], neutrophilia is often accompanied with IgG-mediated immune inflammation [19] and HDM is the most common factor involving in the

pathogenesis of human airway chronic inflammation [3], we hypothesize that HDM-derived factors may be associated with the pathogenesis of neutrophilic inflammation in the airway through inducing the IgG-mediated immune responses. Therefore, in this study, the serum HDM-specific IgG levels in neutrophilic asthma patients were assessed; an antibody against HDM enolase (EnoAb) was generated; the role of EnoAb in the induction of airway neutrophilic inflammation was investigated.

## **Materials and methods**

### **Collection of blood samples from human subjects**

Neutrophilic asthma and eosinophilic asthma patients were recruited into the present study at the Department of Respiriology, First Affiliated Hospital of Guangzhou Medical University (Guangzhou, China). The diagnosis of neutrophilic asthma and eosinophilic asthma was referred to literature [20], in which neutrophilic asthma patients had less than 3% eosinophils and more than 75% neutrophils in the sputum, while eosinophilic asthma patients had more than 3% eosinophils in the sputum. The diagnosis and management of asthma were carried out by our physicians following our routine procedures. Patients with any of the following conditions were excluded: Cancer; other autoimmune diseases; allergic diseases; severe organ diseases; under treatment with immune suppressors for any reasons. Healthy control subjects were also recruited. Blood samples were collected from each human subject through the ulnar vein puncture. The sera were isolated from the blood samples by centrifugation at 4 °C and stored at -80 °C until use. The demographic data of human subjects are presented in Table 1.

### **Anti-Der f EnoAb recognizes airway epithelial cells**

16HBE cells (a human airway epithelial cell line) were fixed with 1% paraformaldehyde for 1 h, exposed to anti-Der f EnoAb or isotype IgG in an Eppendorf for 1 h at room temperature. After washing with phosphate buffered saline (PBS) 3 times, cells were exposed to the second antibody (labeled with FITC) for 30 min and washed with PBS 3 times. The cells were then smeared onto a slide, mounted with cover slips and observed with a confocal microscope.

### **Statistics**

Data were tested for normal distribution by the Kolmogorov-Smirnov test. The difference between two groups was determined by Student *t* test or rank sum test. ANOVA followed by Dunnett's test or Bonferroni test was performed for multiple comparisons. The Spearman correlation assay was performed to show the correlation between data of the two groups.  $P < 0.05$  was set as a significant criterion.

Some experimental procedures are presented in supplemental materials



## Results

### **Serum HDM-specific IgG is correlated with neutrophil numbers in the sputum of patients with neutrophilic asthma**

To determine the association between HDM-derived factors and the pathogenesis of neutrophilic asthma, we collected peripheral blood samples and sputum samples from neutrophilic asthma patients, eosinophilic asthma patients and healthy control (HC) subjects. Serum HDM-specific IgG levels (sIgG, in short), including total sIgG, sIgG1, sIgG2 and sIgG3 were higher in the asthma group than the HC group (Fig. 1A-D). Serum HDM sIgE levels in the neutrophilic asthma group were only slightly higher than HC group (Fig. 1E). The enolase-specific IgG was also detectable in the serum that was significantly more in the neutrophil group than that in the HC group or the eosinophil group (Fig. 1F). Frequency of neutrophils in the sputum was also higher in the asthma group than that in the HC group (Table 1). Positive correlation was identified between sputum neutrophil frequency and serum sIgG levels (including the total sIgG, sIgG1, sIgG2 and sIgG3, respectively) in the neutrophilic asthma patients, but not in the eosinophilic asthma patients (Fig. 1G-J). No apparent correlation was found between serum sIgE levels and sputum neutrophil frequency (Fig. 1K). We also found that sputum eosinophil frequency did not show correlation with or between serum IgG (Fig. S1A-D in the Supplemental Materials). A positive correlation was identified between serum IgE and sputum eosinophil frequency (Fig. S1E). The enolase-specific IgE was detectable in the serum, but there was no significant difference between groups (Fig. S1F). Serum HDM-specific IgG4 levels were higher in the eosinophil group and the neutrophil group as compared with the HC group (Fig. S1G), which did not have correlation with either sputum eosinophil counts or neutrophil counts (Fig. S1H-I). The results demonstrate that the neutrophilic asthma patients have HDM sIgG3 in the serum

that positively correlates with the frequency of sputum neutrophilic frequency.

### **A cross-antibody against HDM-derived enolase recognizes proteins of airway epithelial cells**

We then took a further insight into the role of HDM-derived factors in the pathogenesis of neutrophilic asthma. By whole genome screening, we identified 16,376 genes in HDM (*Dermatophagoides farinae*; Der f) in a previous study [16], in which 2.42% to 8.25% of the Der f genes had identical gene sequences to human genes varying from 50% to 100% (Fig. S2 in supplemental materials). By comparing the enolase gene sequences between Der f and human, we found that the enolase genes have 72% sequence identity (counting the blues) between Der f and human or 71% between Der f and mouse (Fig. S3). The similarity of the enolase gene sequences between Der f and human/mouse prompted us to search the probability that cross-antibodies produced by the human immune system originally against Der f-derived enolase might attack the homologous enolase protein in the human airway tissues. Through the pull-down approach with proteins extracted from 16HBE cells (a human airway epithelial cell line) as baits and analyzed by mass spectrometry (MS). The MS results showed that 89 proteins (including enolase) were captured by the IgG isolated from the sera of asthma patients sensitized to mite (Fig. S4). Previous reports also indicate that enolase involves the pathogenesis of severe asthma [21]. The 16HEB cell-derived enolase could be recognized by anti-Der f antibodies; this was verified by competitive ELISA, in which Der f enolase interfered with the binding between the antibody and human enolase and vice versa (Fig. S5). The serum enolase-specific IgG was higher in the neutrophil group than that in eosinophil group (Fig. 1F). We then assessed the expression of enolase in airway epithelial cells. We found the expression of enolase in both human and mouse airway epithelial cells (Fig. S6). Polyclonal antibodies against Der f-derived enolase were generated and designated

as EnoAb. The EnoAb could specifically bind recombinant enolases (Fig. S5).

### **EnoAb binds airway epithelial cells to form a complex with enolase**

The data of Fig. 1 implicate that EnoAb may be able to bind to the constitutive enolase in body cells. Thus, mice were treated with EnoAb by nasal drops for 3 days. The airway tissues were observed by immunohistochemistry. As expected, EnoAb specifically bound to the airway epithelial cells of mice (Fig. 2A). The results were reproduced in an *in vitro* experiment. By incubating 16HBE cells (a human airway epithelial cell line) with EnoAb for 1 h, we found that EnoAb also bound to 16HBE cells (Fig. 2B). A complex of EnoAb and enolase was detected in the airway tissue protein extracts (Fig. 2C) and the 16HBE cells (Fig. 2D). The results demonstrate that EnoAb can bind to the constitutive enolase to form complexes in airway epithelial cells.

### **EnoAb activates the complement system in airway epithelial cells**

Complements can be produced by several cells, including epithelial cells [22]. The antigen-antibody response can activate the complement system [13]. We then tested the effects of EnoAb interacting with enolase on the activation of complement in airway epithelial cells. Naïve BALB/c mice were treated with nasal drops containing EnoAb daily for 3 days. Bronchial-alveolar lavage fluids (BALF) were collected; the levels of complements in BALF were analyzed by ELISA. The results showed that the levels of C3a, C5a and C5b-9 were significantly higher in samples from mice received EnoAb than those received saline or isotype IgG (Fig. 3A-C). The results were verified by the data of immunohistochemistry, in which the positive staining of C3a, C5a and C5b-9 was localized in airway epithelial cells of the lung tissues (Fig. 3D). The data indicate that, EnoAb can form complexes with enolase and then activate complements on airway epithelial cells. The results were verified with human samples. We collected blood samples from patients with eosinophilic asthma (EA)

and neutrophilic asthma (NA). The plasma was isolated and incubated with either anti-human EnoAb or isotype IgG. The results showed that exposure to EnoAb markedly increased the levels of C3a, C5a and C5b-9 in the plasma in NA samples, but not in EA samples (Fig. 3E-G). Since activation of complement can promote inflammation [23], the data suggest that EnoAb may induce or exacerbate inflammation in the airway.

### **EnoAb induces complement-dependent airway epithelial cell apoptosis**

The data of Fig. 2-3 imply that EnoAb may damage airway epithelial cells. To test the inference, 16HBE cells were exposed to EnoAb in the culture in the presence of human serum (containing complements; Fig. S7) for 6 h. The cells were harvested and analyzed by flow cytometry. The results showed that exposure to EnoAb slightly induced 16HBE cell apoptosis; the presence of complement significantly enhanced the number of apoptotic cells; which was abolished by heat-quenching complements in the serum. Exposure to EnoAb and recombinant C3a also induced the cell apoptosis (Fig. 4A-B). Some apoptotic cells were also PI<sup>+</sup>, indicating these cells had been died. Since dead cells were not detected in control group (Fig. 4A-B), apoptosis is assumed the causative factor to induce these cell dead. On the other hand, mice were treated with EnoAb by nasal drops daily for 6 days. The airway tissue was processed by TUNEL. The results showed that exposure to EnoAb induced airway epithelial cell apoptosis (Fig. 4C). The results demonstrate that exposure to EnoAb can induce airway epithelial cell apoptosis, which can be enhanced by the presence of complements.

### **Exposure to EnoAb impairs the airway epithelial barrier integrity**

To test the effects of EnoAb on the airway epithelial barrier integrity, 16HBE monolayers were prepared and exposed to EnoAb or/and complement-containing serum in the culture. The transepithelial electric resistance (TEER) and permeability to macromolecular tracers

were assessed and used as indicators of epithelial barrier integrity. The results showed that exposure to EnoAb and complement-containing serum markedly impaired the epithelial monolayer integrity manifesting decrease in TEER (Fig. 5A). The results were verified by using the calcium switch technique (Fig. 5B). We also found that exposure to EnoAb and complement-containing serum significantly increased the 16HBE epithelial monolayer barrier permeability. (Fig. 5C). It is noteworthy that the presence of heated serum (in which the compliments were quenched) markedly decreased the effects of EnoAb on impairing the epithelial barrier functions (Fig. 5A-C). On the other hand, after treating mice with nasal drops (containing EnoAb) daily for 6 days, mouse airway epithelial barrier permeability was markedly impaired, which could be blocked by quenching complements with cobra venom factor (CVF) (Fig. 5D). To elucidate if exposure to EnoAb/complement alter the status of tight junction proteins in airway epithelial cells, 16HBE monolayers were collected after exposure to EnoAb/serum overnight and analyzed by RT-qPCR and Western blotting. The results showed that exposure to EnoAb/complement did not apparently alter the levels of ZO-1 in 16HBE cells (Fig. S8). The results indicate that EnoAb together with complements can induce airway epithelial cell apoptosis that compromises the epithelial barrier integrity.

### **Exposure to EnoAb induces neutrophilic inflammation in the airway**

To elucidate if the EnoAb can induce inflammation in the airway, naïve mice were treated with nasal drops containing EnoAb or saline for 6 days. In addition to inducing EnoAb/enolase complexes on the surface of airway epithelium, impairing epithelial barrier integrity, and activation of the complement system as reported in Fig. 2-5, profound inflammatory cell infiltration in the lung tissues was observed (Fig. 6A); hypersensitivity was observed in mice (Fig. 6B); the levels of MPO, MMP9 and total proteins in BALF were significantly higher in the EnoAb group than that in the saline group (Fig. 6C-E) and high

frequency of neutrophils, but not eosinophils, was detected in BALF (Fig. 6F-I) as well as in the lung tissue (Fig. S9). Pretreatment with CVF to quench complements abolished the EnoAb-induced inflammation in the lung (Fig. 6; Fig. S9). The results demonstrate that EnoAb can induce neutrophilic inflammation in the airway.

## Discussion

The present data reveal a novel phenomenon that a cross-antibody, EnoAb, against HDM-derived enolase can initiate neutrophilic inflammation in the airway. Because HDM is the most prevalent allergen involving in the pathogenesis of airway allergic disorder, we investigated the role of EnoAb in the induction of airway inflammation. Most previous studies about HDM-induced airway inflammation focused on the role of IgE and HDM allergens in the pathogenesis of allergic asthma; the present data pinpoint another aspect of HDM, that EnoAb, an IgG antibody, is also involved in the induction of airway inflammation. In line with previous studies, we also found eosinophil infiltration in the airway inflammation induced by EnoAb, while the most conspicuous finding of this study was that the neutrophilic asthma was positively correlated with the serum HDM sIgG levels ( $p < 0.01$ ), although the correlation coefficient is rather low (around 0.3-0.4). Such a phenomenon (the neutrophilic inflammation) was reproduced in the airway tissues of mice by exposing mice to EnoAb, the cross-antibody induced by HDM-derived enolase.

The data show a conspicuous phenomenon that about 50% out of 16,376 mite genes have the similarity to human genes at a variety of range. This feature suggests that some proteins between mite and human are partially similar in the molecular structure. It is known that a protein antigen molecule has many epitopes; each epitope may elicit the generation of a specific antibody [24]. This makes the probability that human immune system producing antibodies against mite antigens may also attack human own tissues. Mite-derived proteins distribute extensively in the human living environment [25], that easily get into the human body through inhalation. Thus, mite-derived proteins contact with human airway tissues constantly and are the most common allergens of airway allergy [26]. Apart from HDM, there are many sources of enolase; *Candida albicans* enolase, for example, has almost the

same sequence identity with HDM and human enolase and the conserved regions are unsurprisingly very much the same [27], as well as non-acarid sources, scabies or food contaminated by mites could be an important source of enolase that might cross react with human tissues. Enolase also exists in fungus, e.g., *Alternaria Alternata* [28]. Fungus-derived molecules are important allergens in the induction of asthma [29]. Thus, the role of enolase from different sources in the pathogenesis of asthma is worth to be further investigated.

The role of HDM-related allergic response in the pathogenesis of asthma has been extensively studied. It is accepted that IgE, mast cells and eosinophils are central effectors in the pathogenesis of asthma attacks [30]. The present data reveal another important factor, the mite-specific IgG is involved in the pathogenesis of mite antigen-related inflammation of the airway tissues. Others also found that asthma patients had mite antigen-specific IgG in the serum [31, 32]. Although some subtypes of IgG, such as IgG1, are beneficial for asthma patients by binding the Fc $\gamma$ RIIB, the IgG inhibitory Fc gamma receptor, to suppress C5a receptor-mediated inflammation [33], the present data show that one of the mite antigen-specific IgGs, EnoAb, has another functional aspect that attacks the enolase of the airway tissues. EnoAb forms a complex with enolase in airway epithelial cells. The complex activates complement and initiates neutrophilic inflammation in the airway. The data also show that the serum HDM-specific IgG3 levels are higher in neutrophil type asthma patients than that in eosinophil-type asthma patients. Among the IgG subtypes, IgG3 has stronger effects on activating complements, while IgG1 mainly works in the IgE production and IgG4 can not activate complement [34]. The complement activation is one of the causative factors in neutrophilic inflammation [13]; our data are in line with this by showing that sputum neutrophil counts are positively correlated with serum sIgG3, whereas no correlation was detected between serum sIgG3 and sputum eosinophil counts since eosinophils are more



relevant to the IgE-mediated allergic inflammation [35].

The present data showed that EnoAb induced airway epithelial barrier dysfunction.

Epithelial barrier dysfunction in the airway mucosa of asthma has been recognized. It is a consensus that the disintegration of epithelial barrier plays an important role in the pathogenesis of airway inflammation [36]. Our early work showed that the dysfunctional epithelial barrier allowed macromolecular substances, such as foreign protein antigens, to penetrate into the deep regions of the mucosa [6], where the foreign antigens gained the opportunity to contact various immune cells to elicit an immune response [37]. A variety of factors have been found to affect epithelial barrier functions, such as psychological stress [38], air pollutions [39], allergic response [40], etc. The present data reveal a novel factor, an cross-antibody against mite-derived enolase, can induce airway epithelial barrier dysfunction.

By directly dropping EnoAb into the airway, we induced airway inflammation in mice, which was characterized by profound infiltration of neutrophils in the lung tissues. This inflammatory type is the same as the neutrophilic asthma, a phenotype of asthma [17].

Neutrophil infiltration in the lung is often associated with the severity of asthma, such as the severe asthma and corticosteroid-resistant asthma [1]. This type of asthma is common in the clinic [17], while its pathogenesis remains to be elusive. The present data provide mechanistic evidence for the explanation of this phenomenon. The mite-derived molecule, the enolase, induces cross-antibodies that may be the important factor to initiate the neutrophilic airway inflammation.

The data can answer to *Witebsky's postulates* for the definition of autoimmune diseases:

Direct evidence of transfer of disease-causing antibody [41]. By treating naïve mice with nasal drops containing EnoAb, neutrophilic inflammation was induced in the lung. In other

words, the mite-derived homologous antigen, enolase, can induce autoimmune disorders in the lung. As aforementioned, we identified 16,376 Der f genes, in which about 50% Der f genes had identical gene sequences of human genes varying from 2% to 100%. Therefore, besides enolase, whether other Der f genes with identical sequences to human are involved with the pathogenesis of human autoimmune diseases following the cross-antibody concept is necessary to be further investigated. Whether all foreign antigens have identical gene sequences of human genes that are associated with autoimmune diseases in human is an interesting research topic and is necessary to be investigated.

We also detected high serum IgE levels in patients with eosinophil asthma subtype. IgE is an important mediator of allergy. By binding the high affinity receptors, IgE can make mast cells sensitized. Re-exposure to specific antigens triggers asthma attacks by activating sensitized mast cells. Administration of anti-IgE antibodies can alleviate asthma attacks or attenuate chronic rhinosinusitis with nasal polyps and nasal allergy [42, 43]. However, not all asthma patients well respond to the anti-IgE therapy [42]. Our data provide mechanistic evidence. The IgE levels were significantly lower in neutrophilic type asthma patients. These asthma patients may not be suitable to be treated with anti-IgE antibodies. The data suggest that treating asthma with anti-IgE antibodies may only be effective in those with high IgE titers [42].

In summary, the present data show that Der f-derived enolase has identical gene sequences at 72% of the sequences of the human enolase gene, which can induce a cross-antibody in the human body. Adoptive transfer with the cross-antibody (generated from mouse) can induce neutrophilic inflammation in the mouse airway mucosa. We conclude that Der f-derived enolase can induce neutrophilic inflammation in the mouse airway.

**Conflict of interest:** None to declare.

**Acknowledgement:** This study was supported by grants from the National Key Research and Development Program on Precision Medicine (No.2016YFC0905802, 2016YFC0903700), Natural Science Foundation of China (31729002, 91542104, 31570932), Science and technology project of Guangdong Province (No.2014B090901041, 2016A020216029), Opening fund of State Key Laboratory of Respiratory Disease (No.SKLRD2016ZJ001), Shenzhen Scientific Technology Basic Research Projects (No.KQTD20170331145453160, JCYJ20160328144536436, KQJSCX20180328095619081), Shenzhen Nanshan District Pioneer Group Research Funds (No.LHTD20180007) and Guangdong Provincial Key Laboratory of Regional Immunity and Diseases (2019B030301009).

**Author contributions:** JL, NH, JLi, XL, QX, CH, DC, LG, KC and DL performed experiments and analyzed data. SKWT provided bioinformatic analysis. J Li provided clinical materials. PCY, ZL and NZ organized the study and supervised experiments. PCY, ZL and JL designed the project. PCY wrote the manuscript. All authors reviewed the manuscript.

## References

1. Ray A, Kolls JK. Neutrophilic Inflammation in Asthma and Association with Disease Severity. *Trends Immunol* 2017; 38(12): 942-954.
2. Globe G, Wiklund I, Mattera M, Zhang H, Revicki DA. Evaluating minimal important differences and responder definitions for the asthma symptom diary in patients with moderate to severe asthma. *J Patient Rep Outcomes* 2019; 3(1): 22.
3. Dullaers M, Schuijs MJ, Willart M, Fierens K, Van Moorlegheem J, Hammad H, Lambrecht BN. House dust mite-driven asthma and allergen-specific T cells depend on B cells when the amount of inhaled allergen is limiting. *J Allergy Clin Immunol* 2017; 140(1): 76-88.e77.
4. Russell RJ, Brightling C. Pathogenesis of asthma: implications for precision medicine. *Clin Sci (Lond)* 2017; 131(14): 1723-1735.
5. Zhu L, Ciaccio CE, Casale TB. Potential new targets for drug development in severe asthma. *World Allergy Organ J* 2018; 11(1): 30.
6. Yang PC, Berin MC, Perdue MH. Enhanced antigen transport across rat tracheal epithelium induced by sensitization and mast cell activation. *J Immunol* 1999; 163(5): 2769-2776.
7. Pawankar R, Yamagishi S, Takizawa R, Yagi T. Mast cell-IgE-and mast cell-structural cell interactions in allergic airway disease. *Curr Drug Targets Inflamm Allergy* 2003; 2(4): 303-312.
8. Sogkas G, Rau E, Atschekzei F, Syed SN, Schmidt RE. The Pyrazole Derivative BTP2 Attenuates IgG Immune Complex-induced Inflammation. *Inflammation* 2018; 41(1): 42-49.

9. Lukacs NW, Glovsky MM, Ward PA. Complement-dependent immune complex-induced bronchial inflammation and hyperreactivity. *Am J Physiol Lung Cell Mol Physiol* 2001; 280(3): L512-518.
10. Schwarz K, Bruckel N, Schwaibold H, von Kleist S, Grunert F. Non-specific cross-reacting antigen: characterization of specific and cross-reacting epitopes. *Mol Immunol* 1989; 26(5): 467-475.
11. Bicova R, Stefan J. Reactivity of antistreptococcus hyperimmune sera with human myocardial tissue. *Zentralbl Bakteriol Mikrobiol Hyg A* 1981; 251(2): 157-164.
12. Delunardo F, Scalzi V, Capozzi A, Camerini S, Misasi R, Pierdominici M, Pendolino M, Crescenzi M, Sorice M, Valesini G, Ortona E, Alessandri C. Streptococcal-vimentin cross-reactive antibodies induce microvascular cardiac endothelial proinflammatory phenotype in rheumatic heart disease. *Clin Exp Immunol* 2013; 173(3): 419-429.
13. Vignesh P, Rawat A, Sharma M, Singh S. Complement in autoimmune diseases. *Clin Chim Acta* 2017; 465: 123-130.
14. Vermeulen N, Arijs I, Joossens S, Vermeire S, Clerens S, Van den Bergh K, Michiels G, Arckens L, Schuit F, Van Lommel L, Rutgeerts P, Bossuyt X. Anti-alpha-enolase antibodies in patients with inflammatory Bowel disease. *Clin Chem* 2008; 54(3): 534-541.
15. Díaz-Ramos A, Roig-Borrellas A, García-Melero A, López-Aleman R.  $\alpha$ -Enolase, a multifunctional protein: its role on pathophysiological situations. *J Biomed Biotechnol* 2012; 2012: 156795.
16. Chan TF, Ji KM, Yim AK, Liu XY, Zhou JW, Li RQ, Yang KY, Li J, Li M, Law PT, Wu YL, Cai ZL, Qin H, Bao Y, Leung RK, Ng PK, Zou J, Zhong XJ, Ran PX, Zhong NS, Liu ZG, Tsui SK. The draft genome, transcriptome, and microbiome of *Dermatophagoides farinae* reveal a broad spectrum of dust mite allergens. *J Allergy Clin Immunol* 2015; 135(2): 539-548.

17. Panettieri RA, Jr. Neutrophilic and Pauci-immune Phenotypes in Severe Asthma. *Immunol Allergy Clin North Am* 2016; 36(3): 569-579.
18. Kwon B, Lee HA, Choi GS, Ye YM, Nahm DH, Park HS. Increased IgG antibody-induced cytotoxicity against airway epithelial cells in patients with nonallergic asthma. *J Clin Immunol* 2009; 29(4): 517-523.
19. Liew PX, Kubes P. The Neutrophil's Role During Health and Disease. *Physiol Rev* 2019; 99(2): 1223-1248.
20. Schleich FN, Zanella D, Stefanuto PH, Bessonov K, Smolinska A, Dallinga JW, Henket M, Paulus V, Guissard F, Graff S, Moermans C, Wouters EFM, Van Steen K, van Schooten FJ, Focant JF, Louis R. Exhaled Volatile Organic Compounds are Able to Discriminate between Neutrophilic and Eosinophilic Asthma. *Am J Respir Crit Care Med* 2019.
21. Nahm DH, Lee KH, Shin JY, Ye YM, Kang Y, Park HS. Identification of alpha-enolase as an autoantigen associated with severe asthma. *J Allergy Clin Immunol* 2006; 118(2): 376-381.
22. Hiemstra PS. Parallel activities and interactions between antimicrobial peptides and complement in host defense at the airway epithelial surface. *Mol Immunol* 2015; 68(1): 28-30.
23. Bakke SS, Aune MH, Niyonzima N, Pilely K, Ryan L, Skjelland M, Garred P, Aukrust P, Halvorsen B, Latz E, Damas JK, Mollnes TE, Espevik T. Cyclodextrin Reduces Cholesterol Crystal-Induced Inflammation by Modulating Complement Activation. *J Immunol* 2017; 199(8): 2910-2920.
24. Potocnakova L, Bhide M, Pulzova LB. An Introduction to B-Cell Epitope Mapping and In Silico Epitope Prediction. *J Immunol Res* 2016; 2016: 6760830.

25. Yu SJ, Liao EC, Tsai JJ. House dust mite allergy: environment evaluation and disease prevention. *Asia Pac Allergy* 2014; 4(4): 241-252.
26. Miller JD. The Role of Dust Mites in Allergy. *Clin Rev Allergy Immunol* 2018.
27. Sundstrom P, Aliaga GR. Molecular cloning of cDNA and analysis of protein secondary structure of *Candida albicans* enolase, an abundant, immunodominant glycolytic enzyme. *J Bacteriol* 1992; 174(21): 6789-6799.
28. Breitenbach M, Simon B, Probst G, Oberkofler H, Ferreira F, Briza P, Achatz G, Unger A, Ebner C, Kraft D, Hirschwehr R. Enolases are highly conserved fungal allergens. *Int Arch Allergy Immunol* 1997; 113(1-3): 114-117.
29. Singh M, Paul N, Singh S, Nayak GR. Asthma and Fungus: Role in Allergic Bronchopulmonary Aspergillosis (ABPA) and Other Conditions. *Indian J Pediatr* 2018; 85(10): 899-904.
30. Galli SJ, Tsai M. IgE and mast cells in allergic disease. *Nat Med* 2012; 18(5): 693-704.
31. Siroux V, Lupinek C, Resch Y, Curin M, Just J, Keil T, Kiss R, Lødrup Carlsen K, Melén E, Nadif R, Pin I, Skrindo I, Vrtala S, Wickman M, Anto JM, Valenta R, Bousquet J. Specific IgE and IgG measured by the MeDALL allergen-chip depend on allergen and route of exposure: The EGEA study. *J Allergy Clin Immunol* 2017; 139(2): 643-654.
32. Kemeny DM, Urbanek R, Ewan P, McHugh S, Richards D, Patel S, Lessof MH. The subclass of IgG antibody in allergic disease: II. The IgG subclass of antibodies produced following natural exposure to dust mite and grass pollen in atopic and non-atopic individuals. *Clin Exp Allergy* 1989; 19(5): 545-549.
33. Pandey MK. Molecular basis for downregulation of C5a-mediated inflammation by IgG1 immune complexes in allergy and asthma. *Curr Allergy Asthma Rep* 2013; 13(6): 596-606.

34. Williams JW, Tjota MY, Sperling AI. The contribution of allergen-specific IgG to the development of th2-mediated airway inflammation. *J Allergy (Cairo)* 2012: 2012: 236075.
35. Stone KD, Prussin C, Metcalfe DD. IgE, mast cells, basophils, and eosinophils. *J Allergy Clin Immunol* 2010: 125(2 Suppl 2): S73-80.
36. Gon Y, Hashimoto S. Role of airway epithelial barrier dysfunction in pathogenesis of asthma. *Allergol Int* 2018: 67(1): 12-17.
37. Yang PC, Jury J, Soderholm JD, Sherman PM, McKay DM, Perdue MH. Chronic psychological stress in rats induces intestinal sensitization to luminal antigens. *Am J Pathol* 2006: 168(1): 104-114; quiz 363.
38. Hattay P, Prusator DK, Tran L, Greenwood-Van Meerveld B. Psychological stress-induced colonic barrier dysfunction: Role of immune-mediated mechanisms. *Neurogastroenterol Motil* 2017: 29(7).
39. An YF, Geng XR, Mo LH, Liu JQ, Yang LT, Zhang XW, Liu ZG, Zhao CQ, Yang PC. The 3-methyl-4-nitrophenol (PNMC) compromises airway epithelial barrier function. *Toxicology* 2018: 395: 9-14.
40. Heijink IH, Nawijn MC, Hackett TL. Airway epithelial barrier function regulates the pathogenesis of allergic asthma. *Clin Exp Allergy* 2014: 44(5): 620-630.
41. Rose NR, Bona C. Defining criteria for autoimmune diseases (Witebsky's postulates revisited). *Immunol Today* 1993: 14(9): 426-430.
42. Mitchell PD, El-Gammal AI, O'Byrne PM. Anti-IgE and Biologic Approaches for the Treatment of Asthma. *Handb Exp Pharmacol* 2017: 237: 131-152.
43. Rivero A, Liang J. Anti-IgE and Anti-IL5 Biologic Therapy in the Treatment of Nasal Polyposis: A Systematic Review and Meta-analysis. *Ann Otol Rhinol Laryngol* 2017: 126(11): 739-747.



## Figure legends

**Figure 1. Sputum neutrophil number is positively correlated with serum HDM specific IgG levels in neutrophilic asthma patients.** Samples of sputum and blood were collected from 41 neutrophilic asthma patients, 42 eosinophilic asthma patients and 30 healthy control (HC) subjects. A-F, scatter plots show serum IgG (A-D), IgE (E) and enolase-specific IgG levels. G-K, scatter dot plots show correlation between serum IgG and sputum neutrophil number (G-J) or serum IgE and sputum neutrophil number (K). Data of neutrophil are presented in Table 1. Data are presented as median with interquartile range (IQR). A positive part was defined as a level 3 standard error above the mean of HC subjects (the area above the shaded region). Statistics: ANOVA + Kruskal Wallis (A-F) and the Spearman correlation assay (G-K). In panel F, recombinant Der f enolase was used in the ELISA experiment to quantify the enolase-specific IgG.

**Figure 2. EnoAb binds airway epithelial cells to form a complex.** A polyclonal antibody (EnoAb) against Der f enolase was generated. a, naïve mice were treated with nasal drops containing EnoAb daily for 3 days. The representative immunohistochemistry images show that EnoAb (in green) binds to the surface of airway epithelial cells (original magnification: ×400). b, 16HBE cells (a human airway epithelial cell line) were fixed with paraformaldehyde first, then incubated with EnoAb for 1 h. The representative immunocytochemistry images show that EnoAb (in green) binds to 16HBE cells (original magnification: ×400). c, the immunoblots show an immune complex of EnoAb and enolase in mouse airway tissue. d, the immunoblots show an immune complex of EnoAb and enolase in 16HBE cells. The data represent 3 independent experiments.

**Figure 3. EnoAb induces complement activation in airway epithelial cells.** Naïve BALB/c mice (6 mice per group) were treated with nasal drops containing EnoAb or isotype IgG daily

for 3 days. a-c, BALF was prepared from each mouse and analyzed by ELISA. Bar graphs show the levels of C3a (a), C5a (b) and C5b-9 (c) in BALF. The lung tissues were examined by immunohistochemistry. D, representative confocal images show the positive staining (in green) of C3a, C5a and C5b-9 in epithelial layers of the lung tissue. The treatment is denoted above each image. The original magnification is  $\times 400$ . E-G, blood samples were collected from 42 patients with eosinophil type asthma (EA) and 41 patients with neutrophil type asthma (NA). The plasmas were isolated from the samples, incubated with anti-human EnoAb (1  $\mu\text{g}/\text{ml}$ ) or isotype IgG for 30 min at 37 °C and analyzed by ELISA. Bar graphs show the levels of C3a (E), C5a (F) and C5b-9 (G). Statistical method: ANOVA followed by the Dunnett's test (A-C) or the Mann Whitney test (E-F).

**Figure 4. Airway epithelial cell apoptosis after exposure to EnoAb and serum.** A, 16HBE cells were exposed to EnoAb or/and serum (containing complement; collected from HC subjects) in the culture overnight. The cells were harvested next day and analyzed by flow cytometry. The gated cells are apoptotic cells. B, the bars present the summarized data of apoptotic cells in panel a. C, naïve BALB/c mice (6 mice per group) were treated with EnoAb or saline daily for 3 days. The lung tissues were examined by TUNEL staining. The apoptotic cells were stained in green (original magnification:  $\times 400$ ). Data of bars are presented as mean  $\pm$  SEM. \* $p < 0.01$ , compared with group I (ANOVA followed by Dunnett's test). Each dot inside bars represent data from one independent experiment. #, heated serum; the complements were quenched. rC3a: Recombinant C3a (100 ng/ml; referred to C3a in the human BALF as presented in Fig. 3A).

**Figure 5. EnoAb induces airway epithelial barrier disintegrate.** A-B, 16HBE cell monolayers were prepared. After reaching confluence, the monolayers were treated with the procedures as denoted in the figures. The curves show the TEER at timepoints as denoted on the x axis.

C, the permeability of 16HBE monolayers was assessed in Transwells. The curves show the permeability of the 16HBE epithelial monolayer barrier. D, naïve BALB/c mice (6 mice per group) were treated with nasal drops containing EnoAb daily for 6 days. The permeability of the airway epithelial barrier was assessed by dextran-absorption. The bars show the permeability of the mouse airway epithelial barrier. The data represent 3 independent experiments and are presented as mean  $\pm$  SEM. The data were analyzed by ANOVA followed by Bonferroni test. #, heated serum; the complements were quenched. CVF: Mice were treated with cobra venom factor (CVF; 200 U/kg, i.p.) 3 days prior to the beginning of nasal drops to deplete complements in mice.

**Figure 6. EnoAb induces airway inflammation.** Naïve BALB/c mice were treated with nasal drops containing saline or EnoAb or isotype IgG daily for 6 days. CVF: Mice received CVF (cobra venom factor; 200 U/kg, i.p., 3 days prior to the beginning of nasal drops). a, representative lung histological images ( $\times 200$ ) show inflammation in the lung of mice treated with EnoAb. b, curves show airway resistance of mice. c-e, bars indicate the levels of MMP9 (c), MPO (d) and total proteins (e) in BALF. f-g, gated dot plots indicate neutrophils (f) and eosinophils (g) in BALF. h-i, bars show the summarized data of neutrophils (h) and eosinophils (i) in BALF. Each group consists of 6 mice. Each dot inside bars present data from one mouse. Statistical method: ANOVA followed by Dunnett test. Each group consists of 6 mice. Data of bars are presented as mean  $\pm$  SEM. Each dot inside bars present data obtained from one mouse.

**Table 1. Demographic and clinical characteristics of recruited subjects**

Subjects' characteristics	Healthy (n=30)	Eosinophilic asthma (n=42)	Neutrophilic asthma (n=41)	p value
Gender (Female:Male)	16/14	25/27	26/25	<0.0001
Age (yr)	38.0 ± 12.3	39.6 ± 12.2	52.3 ± 11.6****#####	<0.0001
Body mass index (Kg/m <sup>2</sup> )	21.1 ± 2.7	21.6 ± 2.8	23.2 ± 3.1#	=0.0087
Smocking history (>10 pack/yr) (%)	0	0	0	-
Age of asthma onset (yr)	-	31.6 ± 13.2	41.0 ± 16.2#	=0.0523
Duration of asthma (yr)	-	7.6 ± 6.8	11.8 ± 15.4	=0.2760
Severe asthma (%)	0	9.5	48.7	<0.0001
Atopy (%)	3.33	57.14	24.39	<0.0001
Total IgE (IU/mL)	46.8 ± 32.7	450.4 ± 556.1**	299.2 ± 718.3	=0.0128
Total IgG (g/L)	12.3 ± 2.1	14.1 ± 3.7	13.0 ± 3.4	=0.1133
Dose of maintenance ICS (BDP; µg/day)	-	385.7 ± 159.7	629.6 ± 229.0#####	<0.0001

ACT	-	19.5 ± 4.4	16.5 ± 4.7#	=0.0375
-----	---	------------	-------------	---------

FeNO (ppb)	18.4 ± 7.2	78.6 ± 58.1****	29.9 ± 22.3###	<0.0001
------------	------------	--------------------	----------------	---------

**Parameters of  
lung function**

FEV1 (L)	3.6 ± 0.7	2.6 ± 0.6****	2.5 ± 0.7****	<0.0001
----------	-----------	---------------	---------------	---------

FEV1 (% predicted)	99.8 ± 8.8	73.5 ± 13.8****	66.5 ± 30.7****	<0.0001
-----------------------	------------	--------------------	-----------------	---------

FVC (L)	4.0 ± 0.9	3.5 ± 0.7	3.2 ± 0.8**	=0.0033
---------	-----------	-----------	-------------	---------

FVC (% predicted)	95.7 ± 7.6	93.9 ± 14.6	88.9 ± 23.1	=0.0344
----------------------	------------	-------------	-------------	---------

FEV1/FVC ratio (%)	93.2 ± 8.0	76.0 ± 11.1****	74.9 ± 16.7****	<0.0001
-----------------------	------------	--------------------	-----------------	---------

PEF <sub>25-75</sub> (L/s)	4.2 ± 0.9	1.8 ± 0.6****	2.2 ± 1.2****	<0.0001
----------------------------	-----------	---------------	---------------	---------

PEF <sub>25-75</sub> (% predicted)	95.8 ± 17.5	39.0 ± 16.3****	23.6 ± 16.5****##	<0.0001
---------------------------------------	-------------	--------------------	-------------------	---------

**Induced sputum**

Eosinophils (%)	0.1 ± 0.3	36.0 ± 23.4****	1.5 ± 1.9####	<0.0001
-----------------	-----------	--------------------	---------------	---------

Neutrophils (%)	34.9 ± 19.0	38.0 ± 18.3	90.4 ± 5.0****####	<0.0001
-----------------	-------------	-------------	--------------------	---------

Macrophage (%)	61.9 ± 19.0	24.4 ± 18.4****	5.9 ± 5.3****####	<0.0001
----------------	-------------	--------------------	-------------------	---------

Lymphocyte (%)	2.1 ± 2.1	0.9 ± 1.2	1.7 ± 1.7	=0.0514
----------------	-----------	-----------	-----------	---------

**Peripheral blood****counts**

Eosinophils (%)	0.1 ± 0.1	0.7 ± 1.1*	0.6 ± 1.3	=0.0256
Neutrophils (%)	3.8 ± 1.3	4.7 ± 2.1	4.9 ± 1.5	P=0.1542

**Combination of****medication**

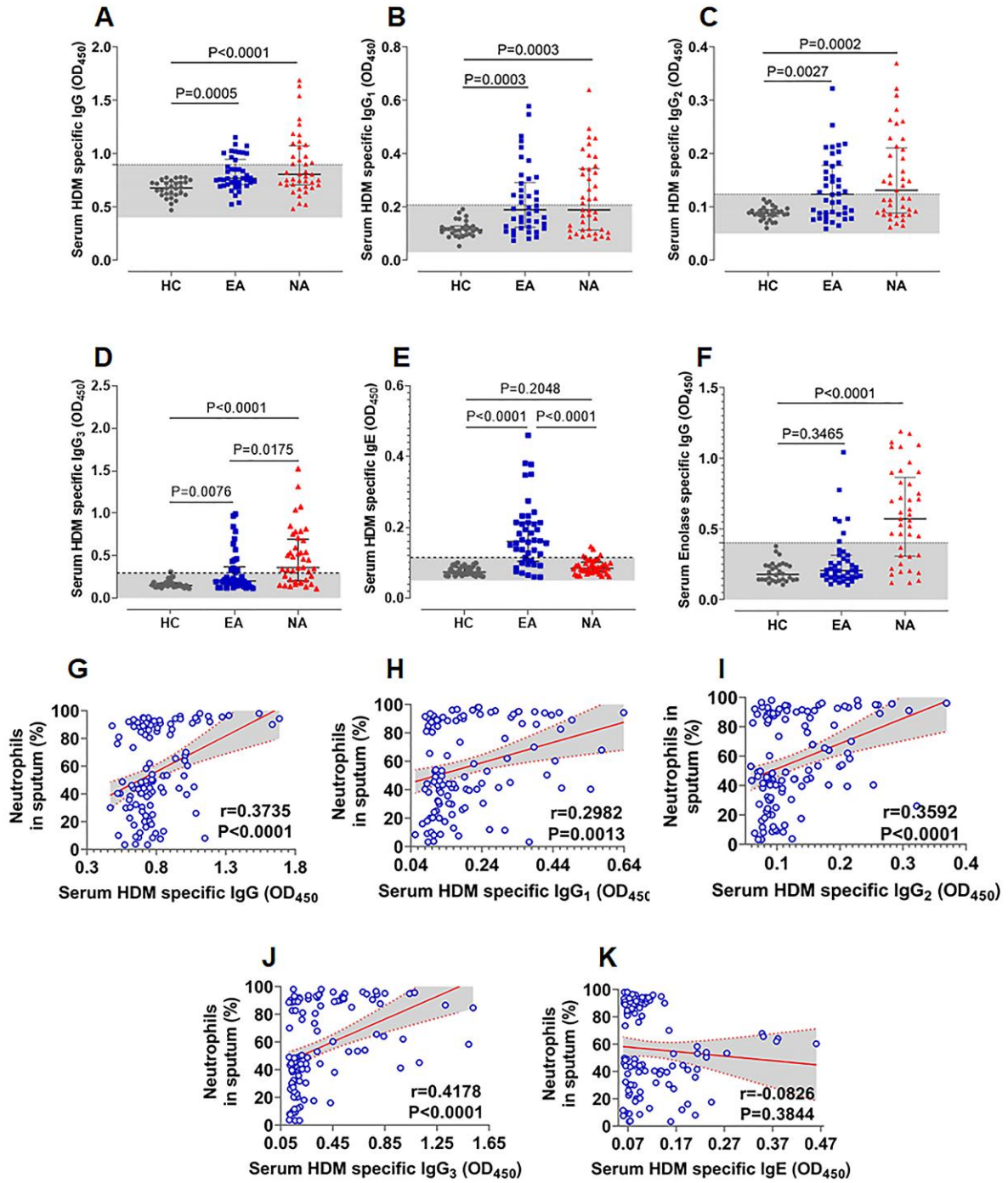
LABA (%)	0	76.1	85.3	<0.0001
Oral CS (%)	0	0	7.3	=0.089
LTRA (%)	0	23.8	14.6	=0.042
Intranasal CS (%)	0	45.2	68.2	<0.001

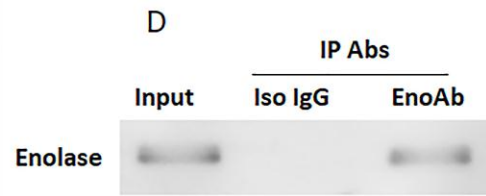
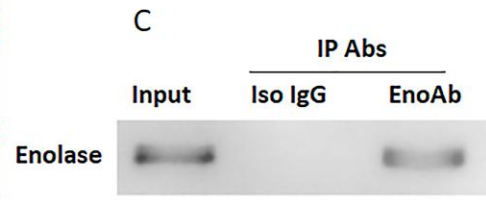
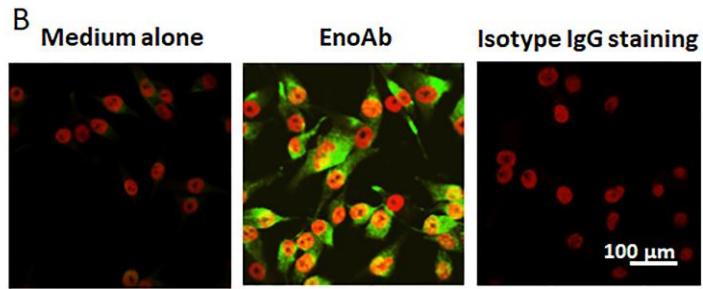
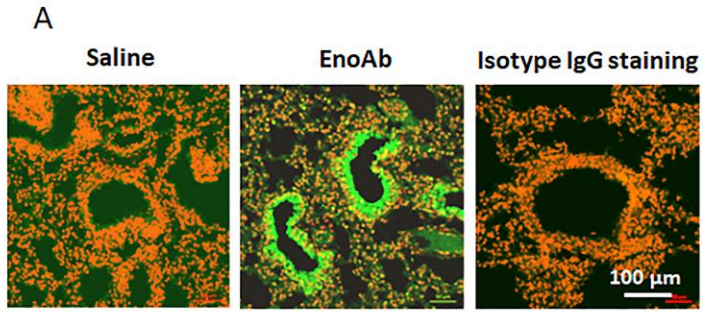
---

Data are shown as means ± SDs. Statistical analysis was performed using the SPSS (version 16.0; IBM, NY, USA).

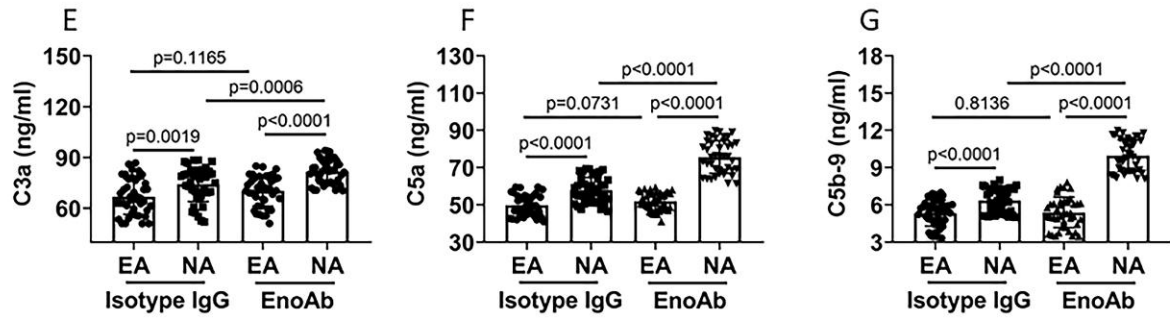
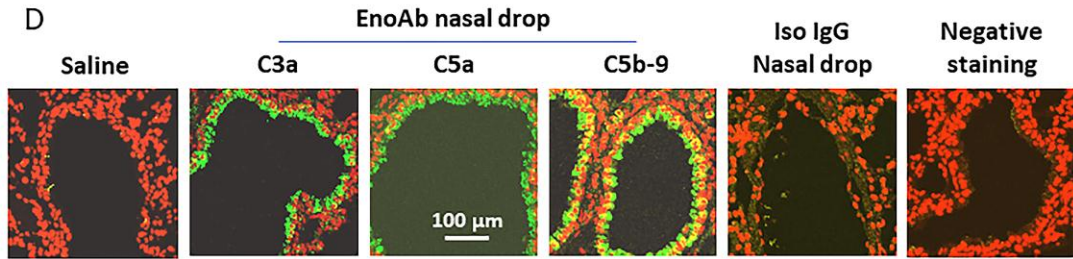
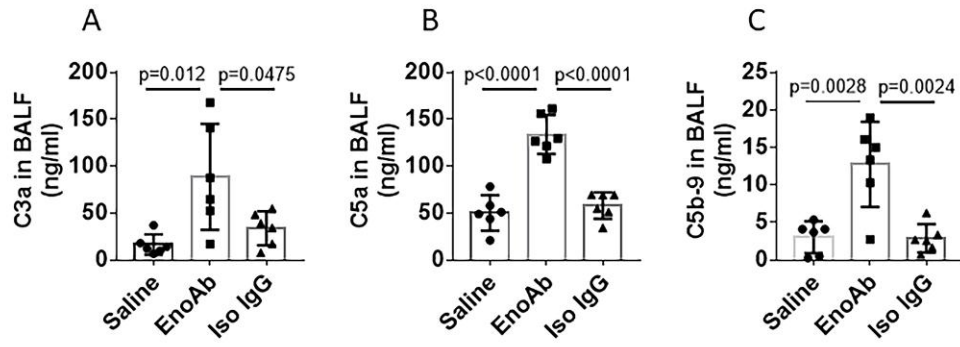
Patients were divided into eosinophilic asthma ( $\geq 3\%$  eosinophils), neutrophilic asthma ( $>76\%$  neutrophils and  $<3\%$  eosinophils) according to the granulocyte count in the sputum. ACT, asthma control test; FeNO, fractional exhaled nitric oxide; FEV<sub>1</sub> forced expiratory volume in 1 sec, FVC forced vital capacity. FEV<sub>1</sub>/FVC, forced expiratory volume in one second to forced vital capacity ratio; PEF<sub>25-75</sub>, forced expiratory flow between 25 and 75% of vital capacity. Atopy, presence of sensitization on SPT (wheal  $\geq 3$ mm) or serum specific IgE ( $\geq 0.35$  kU/L); LABA, long-acting beta-adrenoceptor antagonist; LTRA, leukotriene receptor antagonist.

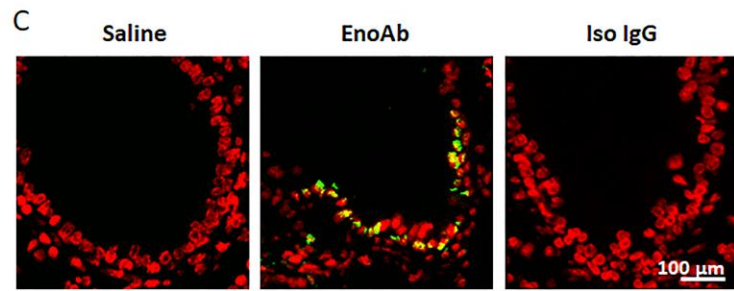
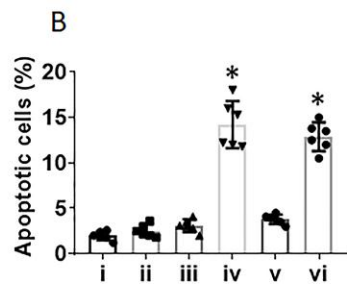
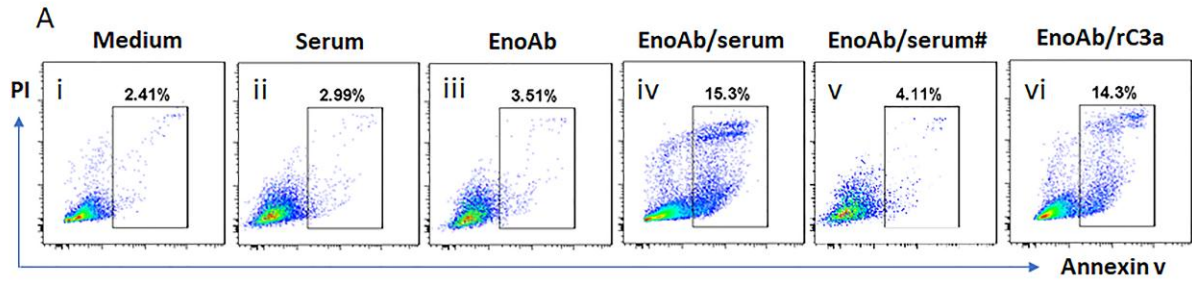
\*P < .05, \*\*P < .01, \*\*\*P < .001 and \*\*\*\*P < .0001 versus healthy subjects. #P < .05, ##P < .01, ###P < .001 and ####P < .0001 versus patients with eosinophilic asthma

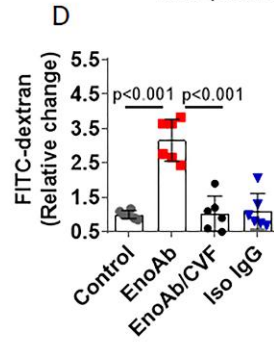
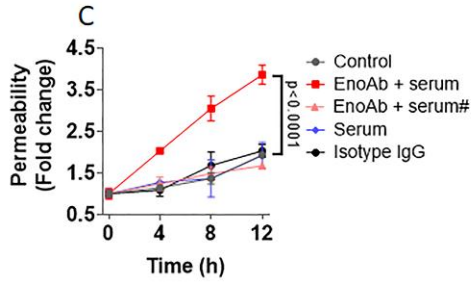
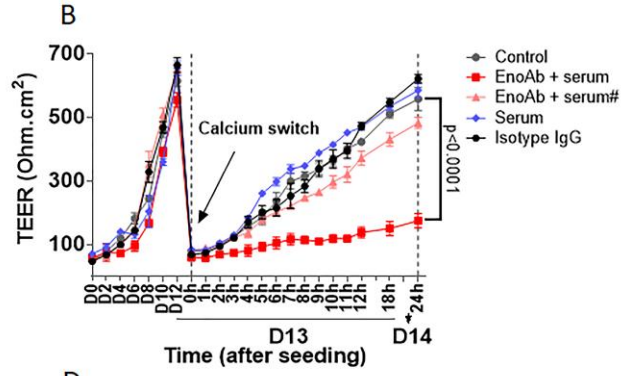
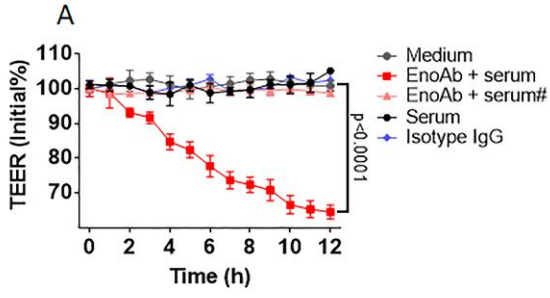


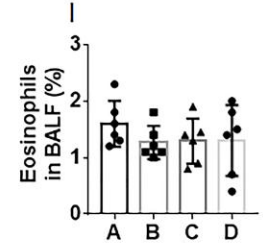
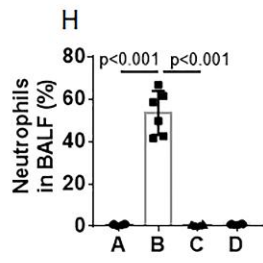
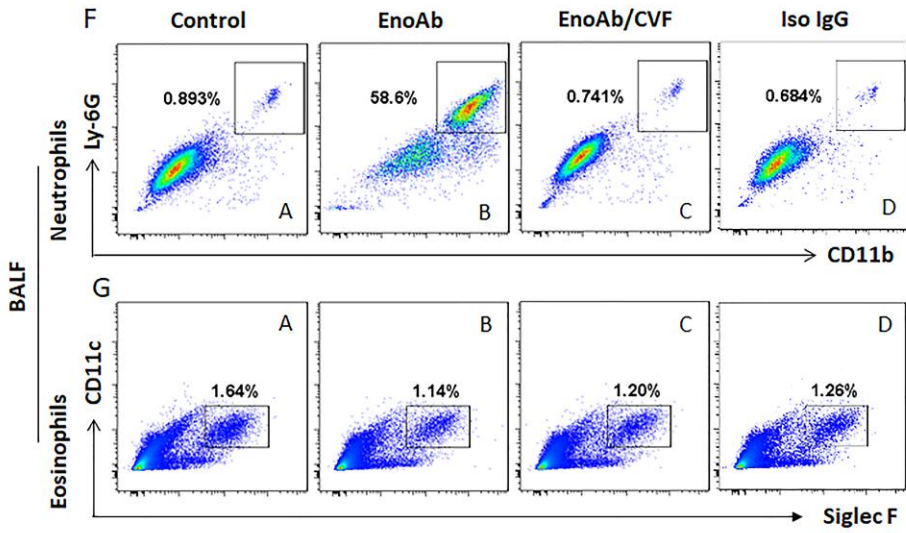
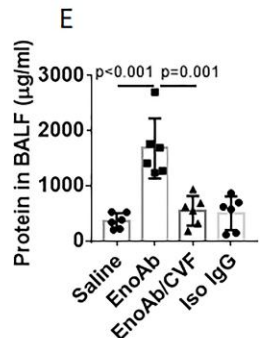
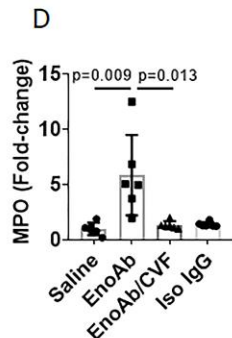
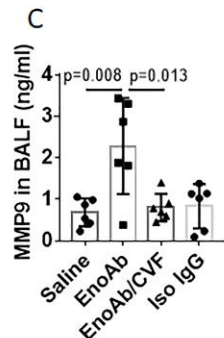
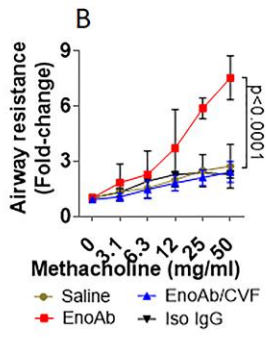
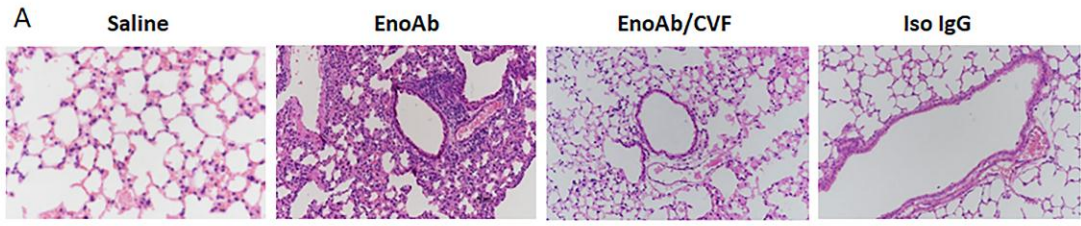












## Supplementary materials

### Reagents

Antibodies against mouse Ly-6G (Cat#. 560599 and 551461), Siglec-F (Cat#. 552126 and 562680), CD11b (Cat#. 557672 and 553310), CD11c (Cat#. 560584) were purchased from BD Biosciences (Franklin Lakes, NJ). Antibody against mouse C5b-9 (Cat#. sc-66190), ZO-1 (sc-33725) and protein G plus-agarose (Cat#. sc-2002) were purchased from Santa Cruz Biotechnology (Santa Cruz, CA). Antibody against mouse CD16/32 (Cat#. 101320) was purchased from BioLegend (San Diego, CA). Mouse control IgG (Cat#. A7028) was purchased from Beyotime Biotechnology (China). Antibody against mouse IgG (Cat#. M04575-1) was purchased from Boster (Beijing, China). Alexa fluor 488-conjugated goat anti-mouse IgG (H+L)(Cat#. GB25301), alexa fluor 488-conjugated goat anti-rabbit IgG (H+L) (Cat#. GB25303), cy3 conjugated goat anti-rabbit IgG (H+L) (Cat#. GB21303) and cy3 conjugated goat anti-mouse IgG (H+L) (Cat#. GB21301) were purchased from Servicebio (Shanghai, China). Goat anti-mouse IgG-HRP (Cat#. 1036-05), goat anti-human IgG-HRP (Cat#. 2015-05), mouse anti-human IgE-HRP (Cat#. 9160-05), mouse anti-human IgG1-HRP (Cat#. 9054-05), mouse anti-human IgG2-HRP (Cat#. 9060-05), mouse anti-human IgG3-HRP (Cat#. 9210-05) and mouse anti-human IgG4-HRP (Cat#. 9200-05) were purchased from Southern Biotechnology (Birmingham, AL). Protein A sepharose FF (Cat#. 17-0780-01) was purchased from GE Healthcare (Pittsburgh, PA). NHS- activated beads 4FF (Cat#. SA039) was purchased from smart-lifesciences (China). FITC-cm-dextran (Cat#. 68059), Freund's adjuvant, complete (Cat#. F5506), Freund's adjuvant, incomplete (Cat#. 101320) were purchased from Sigma-Aldrich (St. Louis., MO). TUNEL apoptosis

assay Kit (Cat#. C1088) was purchased from Beyotime Biotechnology (Shanghai, China). EGTA (Cat#. E8050), RIPA buffer (Cat#. R0020), DAPI solution (Cat#. C0065), Mounting medium, antifading (Cat#. S2100) and Serum of guinea pig (Cat#. S9531) were purchased from Solarbio (Beijing, China). Protein stains K (Cat#. C500021), DNase I (Cat#. A610099), collagenase Type 4 (Cat#. A004210) and poly-L-lysine (Cat#. 25988-63-0) were purchased from Sangon Biotech (Shanghai, China). OCT compound (Cat#. 4583) was purchased from sakura (Torrance, CA). Mouse complement component C5a ELISA Kit (Cat#. CME0066) and mouse myeloperoxidase ELISA Kit (Cat#. CME0115) were purchased from 4A Biotech (Beijing, China). Mouse complement fragment 3a ELISA Kit (Cat#. CSB-E08511m), mouse terminal complement complex C5b-9 ELISA Kit (Cat#. CSB-E08710m) and mouse matrix metalloproteinase 9 ELISA Kit (Cat#. CSB-E08007m) were purchased from Cusabio (Shanghai, China). Confocal dish (Cat#. 801001) was purchased from NEST Biotechnology (USA). Transwell-culture plate inserts (Cat#. 3460) was purchased from Corning (New York, NY). Normal human IgG was purchased from GenScript (Nanjing, China). The recombinant HDM enolase was provided by Shanghai Sangon Biotech (Shanghai, China). The recombinant C3a was purchased from R&D Systems (Minneapolis, MN. Cat#8085-C3-025).

### **Purification of mite specific IgG from serum of patients with asthma**

The total IgG was purified from the serum by protein A referred to published procedures (Gagnon P, Nian R, Lee J, Tan L, Latiff SM, Lim CL, Chuah C, Bi X, Yang Y, Zhang W, Gan HT. Nonspecific interactions of chromatin with immunoglobulin G and protein A, and their impact on purification performance. J Chromatogr A. 2014 May

2;1340:68-78). Mite-specific IgG was further purified from the IgG by affinity chromatography with the sepharose beads absorbed with Der f enolase referred to published procedures (Warren KG, Catz I. Purification of autoantibodies to myelin basic protein by antigen specific affinity chromatography from cerebrospinal fluid IgG of multiple sclerosis patients. Immunoreactivity studies with human myelin basic protein. J Neurol Sci. 1991; 103: 90-6).

### **Generation of mouse Der f enolase-specific IgG (EnoAb, in short)**

Following published procedures (J Immunol. 2014; 193: 2902-10), we generated polyclonal antibodies against Der f enolase through immunizing BALB/c mice. The mice were subcutaneously injected Der f enolase (100 µg/mouse in 1 ml complete Freund adjuvant) at multiple spots on the back. The mice were boosted with Der f enolase (100 µg/mouse) mixed in incomplete Freund adjuvant every other week for 4 times. One week after the last injection, blood was taken from mice through the eyeball pulling. The blood was placed at 4 °C overnight to separate the serum. Total IgG was separated from the serum by protein A. After eluting with an eluting buffer, the Der f enolase specific IgG was separated from the total IgG by passing through affinity chromatography with the sepharose beads absorbed Der f enolase protein. As assessed by ELISA, the generated anti-enolase antibodies well bound recombinant enolases (Fig. S4d).

### **Collection of sputum from human subjects**

Sputum samples were collected from asthma patients and healthy subjects (refer to Table 1 for the demographic data) and processed following published procedures

(Brooks CR, van Dalen CJ, Hermans IF, Gibson PG, Simpson JL, Douwes J. Sputum basophils are increased in eosinophilic asthma compared with non-eosinophilic asthma phenotypes. *Allergy*. 2017 Oct;72(10):1583-1586). The cellular components were analyzed by flow cytometry to assess the frequency of eosinophils and neutrophils (the data are presented in Table 1).

### **Experimental animals**

Male BALB/c mice (6-8 week old), New Zealand rabbits (1-1.5 kg) were purchased from the Guangzhou Experimental Animal Center (Guangzhou, China). Mice and rabbits were maintained at a specific pathogen-free facility with accessing water and food freely. The experimental procedures were approved by the Animal Ethic Committee at Shenzhen University. The experiments were carried out in accordance with the approved guidelines.

### **Preparation of HDM extracts**

The HDM extracts were prepared in our laboratory following our established procedures (Lin J, Huang N, Wang H, Fu Q, Wang E, Li P, Yang L, Luo X, Liu X, Liu Z. Identification of a Novel Cofilin-Related Molecule (Der F 31) as an Allergen From *Dermatophagoides Farinae*. *Immunobiology*; 2018;223:246-251). Proteins were extracted from cells collected from relevant experiments or house dust mites (*D. farina*, maintained in our laboratory) with RIPA lysis buffer (50 mM Tris (pH 7.4), 150 mM NaCl, 1% Triton X-100, 1% sodium deoxycholate, 0.1% SDS, 2 mM sodium pyrophosphate, 25 mM  $\beta$ -glycerophosphate, 1 mM EDTA, 1mM Na<sub>3</sub>VO<sub>4</sub> and protease inhibitor cocktail; from Solarbio Life Science, Beijing, China) following the



manufacturer's instructions. Protein concentrations were determined with Pierce™ BCA Protein Assay Kit. The procedures were carried out at 4 °C.

### **Western blotting**

Proteins were fractionated by SDS-PAGE (Sodium dodecyl sulfate-Polyacrylamide gel electrophoresis) and transferred onto a PVDF membrane. After blocking with 5% skim milk for 30 min, the membrane was incubated with the primary antibodies of interest overnight at 4 °C, washed with TBST (Tris-buffered saline containing 0.1% Tween 20) 3 times, incubated with peroxidase-labeled secondary antibodies for 2 h at room temperature, washed with TBST 3 times. The immunoblots on the membrane were developed with the enhanced chemiluminescence and photographed in an imaging station.

### **Enzyme-linked immunosorbent assay (ELISA)**

Levels of cytokines or proteins in the serum or BALF were determined by ELISA with purchased reagent kits following the manufacturer's instructions.

### **Cell culture**

Immune cells were cultured with RPMI1640 medium. Epithelial cells were cultured with Dulbecco's Modified Eagle's medium. The medium was supplemented with 10% fetal bovine serum, 100 U/ml penicillin, 0.1 mg/ml streptomycin and 2 mM glutamine. Medium was changed in 2-3 days. Cell viability was greater than 99% as assessed by Trypan blue exclusion assay.

### **Immunohistochemistry**

Lung tissues were snap frozen in liquid nitrogen. Cryosections were prepared and fixed with cold acetone for 20 min. After blocking with 1% bovine serum albumin (BSA), sections were incubated with the first antibodies of interest or isotype IgG overnight at 4 °C, washed with PBS 3 times, incubated with secondary antibodies (labeled with fluorescence) for 2 h at room temperature and washed with PBS 3 times. The sections were mounted with cover slips and observed with a confocal microscope.

### **TdT-mediated dUTP Nick-End Labeling (TUNEL)**

Cryosections of airway tissue were prepared and stained with TUNEL with a commercial reagent kit following the manufacturer's instructions. The sections were observed with a confocal microscope.

### **Immunoprecipitation (IP)**

Proteins were precleared by incubating with protein G agarose beads for 2 h. The beads were removed by centrifugation at 5,000 g for 5 min. The supernatant was incubated with antibodies of interest or isotype IgG overnight at 4 °C to form immune complexes. The complexes were precipitated by incubating with protein G agarose beads for 2 h. The beads were collected by centrifugation at 5,000 g for 5 min. Proteins on the beads were eluted with an eluting buffer and analyzed by Western blotting.

### **Assessment of apoptotic cells**

Cells were collected from relevant experiments and stained with propidium iodide (PI) and annexin v following the manufacturer's instructions. Cells were analyzed by flow cytometry. Data were processed with flowjo software package. Cells stained annexin v<sup>+</sup> or both annexin v<sup>+</sup> PI<sup>+</sup> were regarded apoptotic.

### **Assessment of the effects of EnoAb on airway epithelial barrier functions**

16HBE cells were cultured into monolayer in a Transwell system. Upon confluence, EnoAb was added to upper chambers at 0.02% in total volume together with complement-containing serum or heated serum (the complement was quenched) at 10 µl/ml. The transepithelial electric resistance (TEER) of the monolayers was recorded every 2-h from 0-12 h. To assess the permeability of the monolayers, FITC-dextran (MW = 40 kDa) was added to upper chambers at 10 µg/ml. Samples (0.1 ml) were taken from basal chambers every 4 h from 0-12 h. Levels of FITC in the samples were determined by fluorescent spectrometry. The effects of anti-Der f enolase IgG on the function of intercellular junction complex was also tested with the calcium-switch following published procedures (Tobey NA, Argote CM, Hosseini SS, Orlando RC. Calcium-switch technique and junctional permeability in native rabbit esophageal epithelium. *Am J Physiol Gastrointest Liver Physiol.* 2004; 286: G1042-9). Briefly, after reaching confluence, 16HBE monolayers were exposed to calcium-free medium; the TEER then dropped progressively until a plateau was reached (in about 2 h). The medium was then replaced with a calcium-containing medium. TEER of the monolayer was recorded every hour from 0 to 12 h.

To test the effects of EnoAb on airway epithelial barrier function *in vivo*, mice received nasal drops (25  $\mu$ l/nostril/time) containing EnoAb (1  $\mu$ g/ml) daily for 6 days. On day 7, mice were treated with nasal drops containing FITC-dextran (10 mg/kg; in 25  $\mu$ l/nostril; PLoS One. 2014;9:e101925). Mice were sacrificed 3 h later. Blood was collected from each mouse. The serum was isolated. Levels of FITC-dextran in the serum were determined by fluorescent spectrometry. To elucidate the role of complements in the EnoAb on the airway epithelial barrier dysfunction, mice were treated with cobra venom factor (CVF; 200 U/kg, i.p.) 3 days prior to the beginning of nasal drops to deplete complements in mice.

#### **Real-time quantitative RT-PCR**

16HBE cells were collected from the barrier function experiments. The total RNA was extracted from the cells with the TRIzol reagents, converted to cDNA with a QuantiTect Reverse Transcription Kit (Qiagen) following the manufacturer's instruction. The samples were amplified in a qPCR device (CFX96 Touch Real-Time PCR Detection System) with the SYBR Green Master Mix (Invitrogen) and the presence of ZO-1 primers (tcagagtggggaaacgtcaa and tggttcaggatcaggacgac). The results were calculated by the  $2^{-\Delta\Delta Ct}$  method and presented as relative change.

#### **Flow cytometry**

Cells were collected from relevant experiments. In the surface staining, cells were stained with antibodies of interest (labeled with fluorescence) or isotype IgG for 30 min at 4 °C. In the case of intracellular staining, cells were fixed using 1% paraformaldehyde, permeabilized with perm buffer (0.5% saponin) and stained with

antibodies of interest (labeled with fluorescence) or isotype IgG for 30 min at 4 °C. The cells were analyzed with a flow cytometer (FACSCanto II). Data were processed using flowjo with the data of isotype IgG staining as gating references.

### **Development of airway inflammation in mice with EnoAb**

BALB/c mice (6 per group) were treated with nasal drops containing EnoAb (1 µg/ml) daily for 6 days. On day 7, the airway hyperresponsiveness to methacholine was measured with the unrestrained whole-body plethysmography. Bronchoalveolar lavage fluid (BALF) was collected from each mouse by infusion and extraction of 1 ml of ice-cold PBS. The procedure was repeated 3 times, and the lavage fluids were pooled and centrifuged at 1,000 g for 10 min. The supernatant was collected and analyzed by ELISA. The cell pellets were resuspended in culture medium and analyzed by flow cytometry. A piece of lung tissue was excised and fixed with 4% formalin. Paraffin sections were prepared and stained with hematoxylin and eosin. The sections were observed under a light microscope.

### **Competitive ELISA to verify the binding specificity between homo (or Der f) enolase and EnoAb**

In order to validate the cross-reactions between Der f enolase and Homo enolase, pooled sera from patients were used for inhibition assay. Firstly, sera were diluted for 20 times in PBS which containing 2% BSA and 0.05% Tween 20 and then subsequently added with Der f enolase (final concentration: 0.0002, 0.002, 0.02, 0.2, 2g/ml) or Homo enolase at 4°C for pre-incubated overnight. After that, the sera were then added to the microtiter plates pre-coated with Homo enolase or Der f enolase

(0.1 µg/well). Three parallel measurements were performed in each group and the inhibition rates were calculated in accordance to the formula:  $\text{Inhibition (\%)} = \frac{\text{OD}_0 - \text{OD}_i}{\text{OD}_0 - \text{OD}_{\text{BSA}}}$ . Where the  $\text{OD}_0$  is the original optical density of antigen without inhibitor added; and  $\text{OD}_i$  is the optical density of antigen after inhibitor adding; and  $\text{OD}_{\text{BSA}}$  is the optical density with no inhibitor but BSA adding.

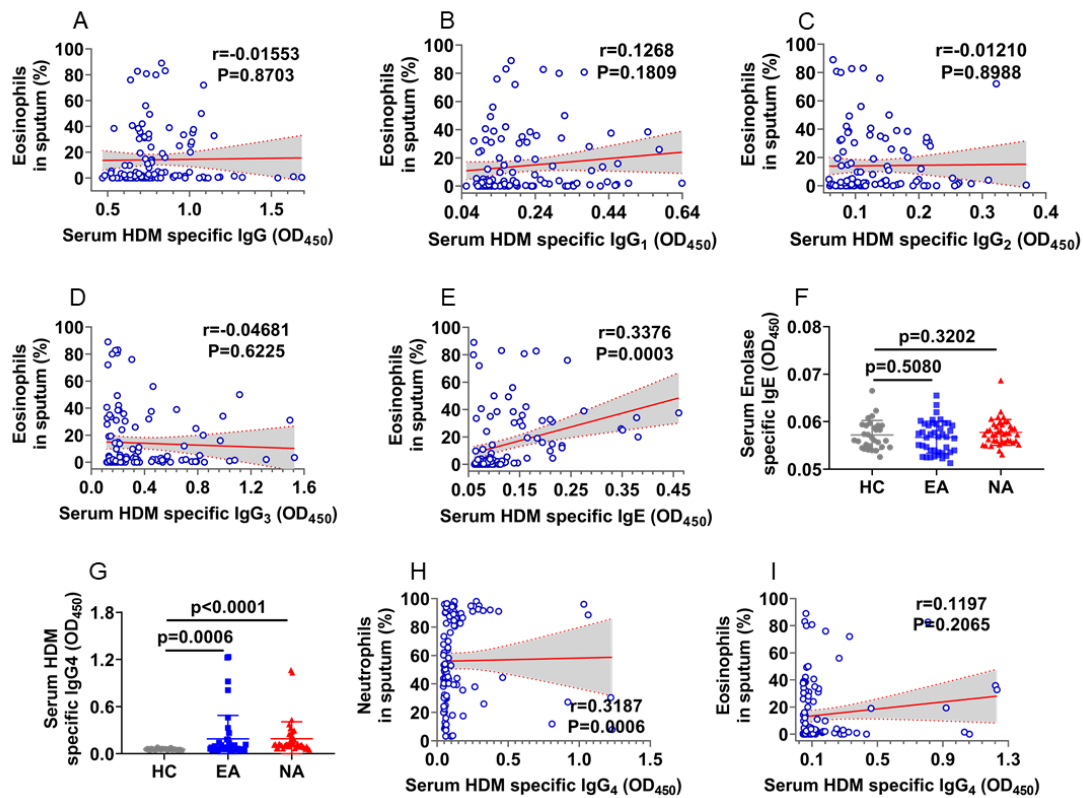


**Figure S1. Supplementary data to Figure 1 in the main text.** Samples of sputum and blood were collected from 41 neutrophilic asthma patients, 42 eosinophilic asthma patients and 30 healthy control (HC) subjects. a-e, scatter plots show correlation between serum IgG (a-d) or IgE (e) levels and sputum eosinophil frequency. F, serum enolase-specific IgE levels. G, serum HDM-specific IgG4 levels. H-I, no correlation between serum HDM-specific IgG4 and sputum neutrophil counts or eosinophil

counts. Statistics of F and G: the Mann Whitney test. A-E, H-I, the Spearman correlation assay.

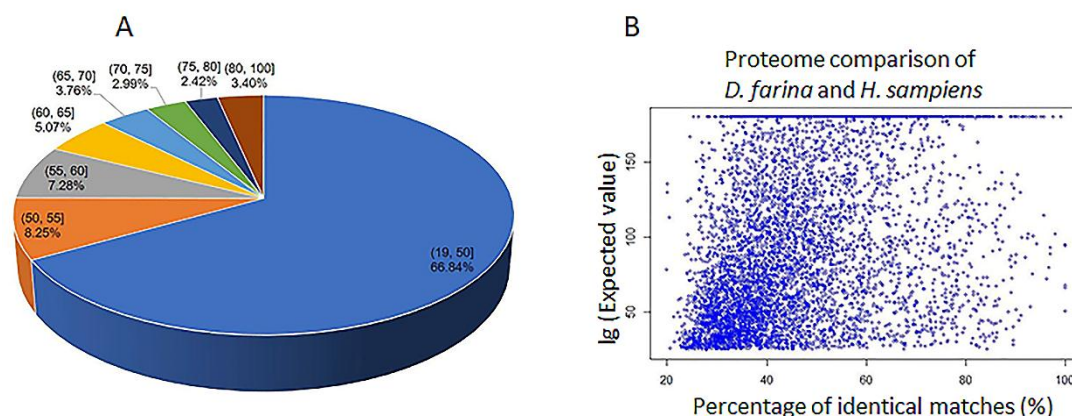


**Figure S2. Gene sequence identical matches between Der f and human.** The proteome of *H. sapiens* (20,399 proteins, last modified on Dec. 13, 2018) was downloaded from UniProt database and the proteome of *D. farinae* (18,087 proteins) was provided by Prof. Stephen Kwok-Wing Tsui's lab (Chan, T.-F., et al., *The draft genome, transcriptome, and microbiome of Dermatophagoides farinae reveal a broad spectrum of dust mite allergens. Journal of Allergy and Clinical Immunology, 2015. 135(2): p. 539-548*). NCBI Blast p 2.6.0+ program was used to compare the proteomes of *D. farinae* and *H. sapiens*, in which the expect value cutoff was set at  $1e-25$ , 1 max\_hsp and 1 max\_target\_seqs were set. a, the distribution of the percentage of identical matches in the Blastp results. Among the 6,329 *D. farinae* proteins that shared high similarities to *H. sapiens* proteins, the lowest percentage of identical matches of is 19.89%, 2,113 proteins (33.16%) have  $\geq 50\%$  percentage of identical matches and 559 proteins (8.80%) have  $\geq 70\%$  percentage of identical matches. b, the distribution of Blastp results of *D. farinae* and *H. sapiens* proteomes.

Among the 18,087 annotated proteins of *D. farinae*, 6,329 proteins shared high similarities to 4722 *H. sapiens* proteins. The minimum of expect value was set at 1e-180.

```

Der_f_enolase MSTLRTIARQIFDSRGNPTIEVDLITDFCVFRAAVPSGASTGTIEALELRDADKAHYHGKSVLKATANVNDVLPAPLISQGLDVTKQKEI 90
Homo_enolase MSTLRTIAREIFDSRGNPTIEVDLFTSKGLFRAAVPSGASTGTIEALELRDADKTRVMGRGVSKAVEHINKTIAPALVSKKLVITECEKI 90
Mouse_enolase MSTLRTIAREIFDSRGNPTIEVDLITAKGLFRAAVPSGASTGTIEALELRDADKTRFMGRGVSCAVEHINNTIAPALVSKKLVVTECEKI 90
Consensus msi i ar ifdsrgnpt evdl t g fraavpsgastgi ealelrd dk gk v a n iap l s v q i
Der_f_enolase DDLITQLDNTFNKQNLGNAILGVSLAVKAGAAKRVPLVQHISDLADIKFVLPVPFNFVINGGSHAGNRLAMQEFMILFTGASSFTIE 180
Homo_enolase DKLITEMDCITENKSKFCANAILGVSLAVCKAGAVKCVPLVYRHITADLAGNSEVILPVPFNFVINGGSHAGNRLAMQEFMILFVGAANFRE 180
Mouse_enolase DKLITEMDCITENKSKFCANAILGVSLAVCKAGAVKCVPLVYRHITADLAGNSEVILPVPFNFVINGGSHAGNRLAMQEFMILFVGAANFRE 180
Consensus d l i d t n k g n a i l g v s l a v k a g a k r v p l y h i d l a e l p v p a f n v i n g g s h a g n r l a m q e f m i l p g a f e
Der_f_enolase AMKVGSEVYHLLKNVIRQRVGDATVGDDEGGFAPNINQNKBAUDDIMSTIQAGYSGKIDIGMDVAASEFVREGKYDLDLDFKNANSDKSA 270
Homo_enolase AMRIGAEVYHLLKNVIRERYGRDATVGDDEGGFAPNILENKEGUELLKTIATKAGYTDKVVIGMDVAASEFVREGKYDLDLDFKSPDDPSR 269
Mouse_enolase AMRIGAEVYHLLKNVIRERYGRDATVGDDEGGFAPNILENKEAUELLKTIATKAGYTDQVVIIGMDVAASEFVREGKYDLDLDFKSPDDPSR 269
Consensus a m g e v y h l l k n v i r q r v g d a t v g d e g g f a p n i n k e b a u d d i m s t i q a g y s g k i d i g m d v a a s e f v r e g k y d l d l f k n a n s d k s a
Der_f_enolase WLEPSQLADLYRCHVYKDYPTVSIEDPPDQDWDWDTAFTSSVSGQVVGDDLTVTNPKRIQTAAERKICNCLLLKVNQIGSVTESLQACKL 360
Homo_enolase YISFDQLADLYKSFYKDYPTVSIEDPPDQDWDGAWQKFTASAGIQVVGDDLTVTNPKRIATAVNERSCNCLLLKVNQIGSVTESLQACKL 359
Mouse_enolase YISFDQLADLYKSFYKDYPTVSIEDPPDQDWDGAWQKFTASAGIQVVGDDLTVTNPKRIATAVNERSCNCLLLKVNQIGSVTESLQACKL 359
Consensus w l e p s q l a d l y r c h v y k d y p t v s i e d p p d q d w d w d t a f t s s v s g q v v g d d l t v t n p k r i q t a a e r k i c n c l l l k v n q i g s v t e s l q a c k l
Der_f_enolase ARSNGWGMVSHRSGETEDTFIADLVVGLCTGQIKTGAPCRSERLAKYNQLRIIEEELGAKAKYACKFRFFI 433
Homo_enolase AQANGWGMVSHRSGETEDTFIADLVVGLCTGQIKTGAPCRSERLAKYNQLRIIEEELGSKARFAGRFRNPLA 433
Mouse_enolase AQANGWGMVSHRSGETEDTFIADLVVGLCTGQIKTGAPCRSERLAKYNQLRIIEEELGSKARFAGRFRNPLA 433
Consensus a r s n g w g m v s h r s g e t e d t f i a d l v v g l c t g q i k t g a p c r s e r l a k y n q l r i e e e l g a k a k y a c k f r f f i

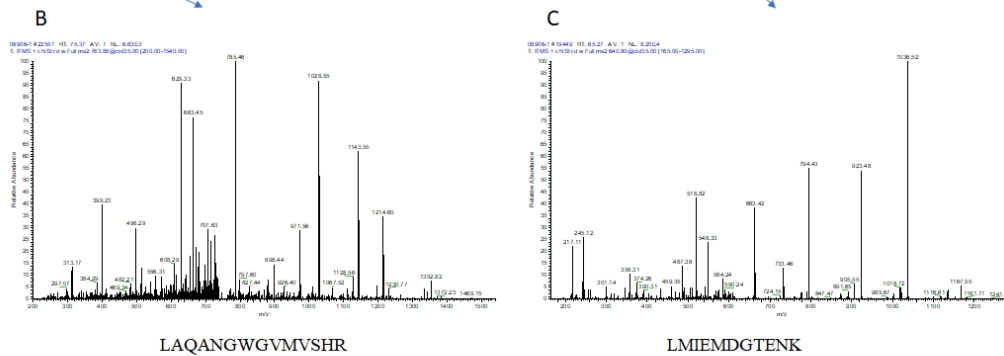
```

**Figure S3. Amino acid sequence alignment of enolase between Der f and human or mouse.** The enolase gene sequence was obtained from the Gene Bank (Der f: AHV90299.1; human: NP\_001419.1; mouse: XP\_021056757.1) and analyzed by the software of Basic Local Alignment Search Tool BLAST (<https://blast.ncbi.nlm.nih.gov/Blast.cgi>) and DNAMAN software (Lynnon 6BioSoft, Vandreuil, Canada). The table show the similarity (with the blue background) between Der f and human (72%), Der f and mouse (71%) and human and mouse (95%).



A

1 MSILKIHARE IFDSRGNPTV EVDLFTSKGL FRAAVPSGAS TGIYEALELR DNDKTRYMGK  
 61 GVSKAVEHIN KTIAPALVSK KLVNTEQEKI DKLMIEMDGT ENKSKFGANA ILGVSLAVCK  
 121 AGAVEKGVPL YRHIADLAGN SEVILPVPF NVINGGSHAG NKLAMQEFMI LPVGAANFRE  
 181 AMRIGAEVYH NLKNVIKEY GKDATNVGDE GGFAPNILEN KEGLELLKTA IGKAGYTDKV  
 241 VIGMDVAASE FFRSGKYDLD FKSPDDPSRY ISPDQLADLY KSFIKDYPVV SIEDPFDQDD  
 301 WGAWQKFTAS AGIQVVGDDL TVTNPKRIAK AVNEKSCNCL LLKVNQIGSV TESLQACKLA  
 361 QANGWGMVS HRSGETEDTF IADLVVGLCT GQIKTGAPCR SERLAKYNQL LRIIEELGSK  
 421 AKFAGRNFRN PLAK



MS parameters of enolase

**Figure S4. MS analysis of enolase protein extracted from 16HBE cells recognized by mite-specific IgG**

a, the enolase amino acid sequence. b-c, MS parameters of enolase, which are pointed by arrows of enolase amino acid sequence fragments (in red color). The procedures of MS are listed below:

1. Samples are re-suspended with Nano-RPLC buffer A.
2. The online Nano-RPLC was employed on the Eksigent nanoLC-Ultra™ 2D System (AB SCIEX). The samples were loaded on C18 nanoLC trap column (100µm×3cm, C18, 3µm, 150Å) and washed by Nano-RPLC Buffer A(0.1%FA, 2%ACN) at 2µL/min for 10 mins.
3. An elution gradient of 5-35% acetonitrile (0.1%formic acid) in 90 mins gradient was used on an analytical ChromXP C18 column (75µm x 15 cm, C18, 3µm 120 Å) with spray tip.
4. Data acquisition was performed with a Triple TOF 5600 System (AB SCIEX, USA)

fitted with a Nanospray III source (AB SCIEX, USA) and a pulled quartz tip as the emitter (New Objectives, USA). Data were acquired using an ion spray voltage of 2.5 kV, curtain gas of 30 PSI, nebulizer gas of 5 PSI, and an interface heater temperature of 150°C. For information dependant acquisition (IDA), survey scans were acquired in 250 ms and as many as 35 product ion scans were collected if they exceeded a threshold of 150 counts per second (counts/s) with a 2+ to 5+ charge-state. The total cycle time was fixed to 2.5s. A rolling collision energy setting was applied to all precursor ions for collision-induced dissociation (CID). Dynamic exclusion was set for ½ of peak width (18 s). And the precursor was then refreshed off the exclusion list. Based on combined MS and MS/MS spectra, proteins were successfully identified based on 95% or higher confidence interval of their scores in the MASCOT V2.3 search engine (Matrix Science Ltd., London, U.K.), using the following search parameters: cow- lacobacillus casel mix database. trypsin as the digestion enzyme. two missed cleavage sites. fixed modifications of Carbamidomethyl (C). partial modifications of Acetyl (Protein N-term), Deamidated (NQ), Dioxidation (W), Oxidation (M) Phospho (ST) and Phospho (Y) ± 15ppm for precursor ion tolerance and ± 0.15Da for fragment ion tolerance.

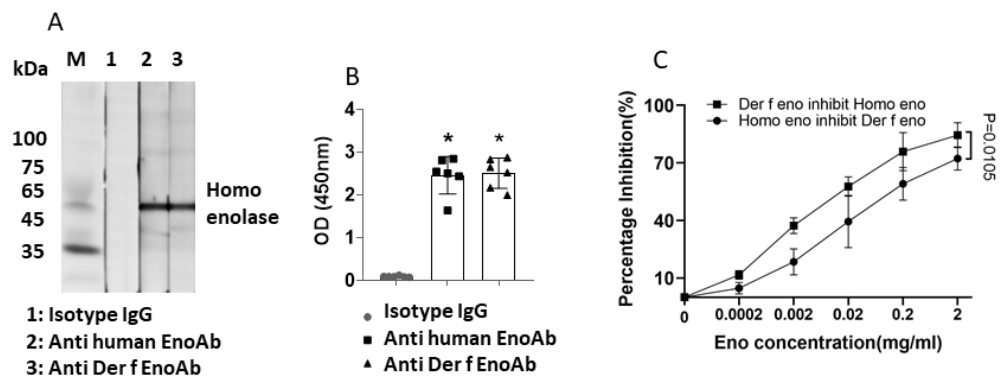


**Figure S5. Mite-derived enolase-specific IgG (EnoAb) binds enolase derived from airway epithelial cells.** Enolase protein was purified from 16HBE cells and analyzed by immunoblotting and ELISA using EnoAb of both human- and Der f-sources. A, a polyclonal antibody against human enolase or Der f enolase was generated and designated as EnoAb. The immunoblots show the EnoAb binds recombinant human enolase or Der f enolase. B, ELISA results show EnoAb specifically binds human enolase and Der f enolase. C, competitive results. The upper curve shows the inhibitory effects of Der f enolase (eno, in short) on the binding between homo eno and EnoAb. The lower curve shows the inhibitory effects of homo eno on the binding between Der f eno and EnoAb. The data represent 3 independent experiments. Statistical method: ANOVA. Iso: Isotype.

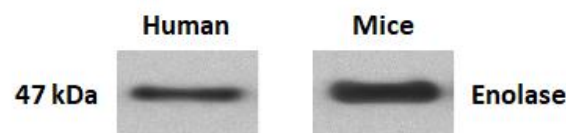


**Figure S6. Human and mouse airway epithelial cells express enolase.** Proteins were extracted from human airway epithelial cell line, 16HBE cells and mouse lung tissue. The proteins were analyzed by Western blotting with anti-human enolase or anti-mouse enolase antibody, respectively. The immunoblots show positive staining of enolase in samples from 16HBE cells and mouse lung tissue.

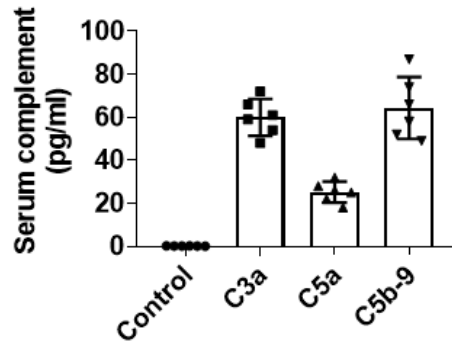


**Figure S7. Healthy subject serum complement levels.** Blood samples were collected from 6 healthy subjects. The serum was isolated from the samples and analyzed by ELISA. The bars show serum complement levels (mean  $\pm$  SEM). Control: Saline was added to the wells instead of serum samples. Each dot presents data obtained from one sample.

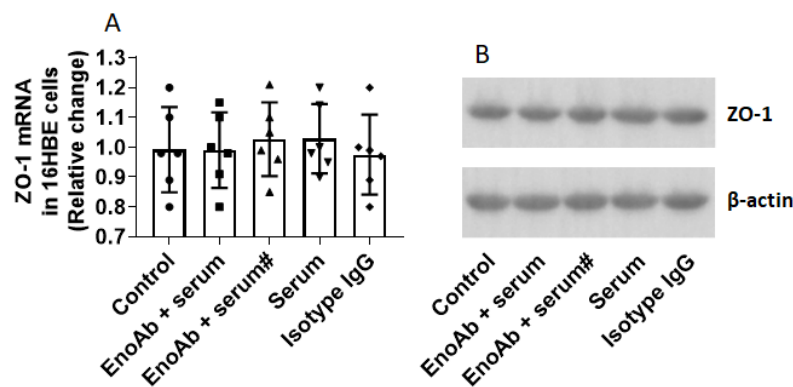


**Figure S8. Assessment of the effects of EnoAb+serum on ZO-1 expression in 16HBE cells.** The same as the description of Fig. 5 in the main text, 16HBE cell monolayers were prepared. After reaching confluence, the monolayers were treated with the procedures as denoted on the x axis of the bar graphs. The cells were collected on next day and analyzed by RT-qPCR and Western blotting. A, bars show ZO-1 mRNA levels in 16 HBE cells. B, immunoblots show ZO-1 protein levels in 16 HBE cells. The data of bars are presented as mean  $\pm$  SEM. Each dot presents data obtained from

one sample. The immunoblots are from one experiment that represent 6 independent experiments. The data were analyzed by ANOVA. #, heated serum; the complements were quenched.

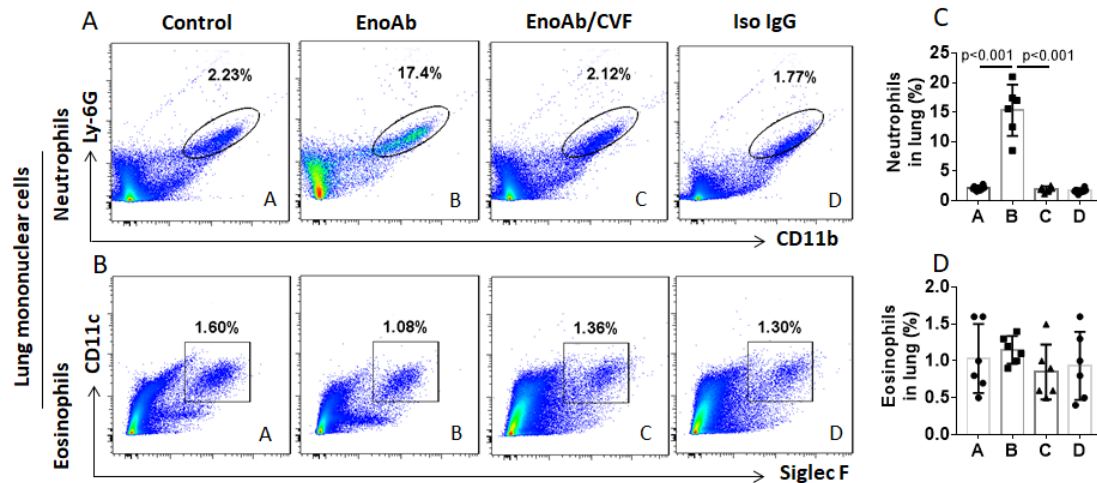


**Figure S9. EnoAb induces neutrophil infiltration in the lung.** Naïve BALB/c mice were treated with nasal drops containing EnoAb daily for 3 days. CVF: Mice received CVF (cobra venom factor; 200 U/kg, i.p., 3 days prior to the beginning of nasal drops). After sacrifice, the lung was excised. Mononuclear cells were isolated from the lung tissue and analyzed by flow cytometry. a-b, the gated dot plots show the frequency of neutrophils (a) and eosinophils (b) in the mononuclear cells. c-d, bars indicate the summarized neutrophils (c) and eosinophils (d) in the gated cells of a and b. Each dot inside bars present data obtained from one mouse. Data of bars are presented as mean  $\pm$  SEM. Each group consisted of 6 mice. Statistics: ANOVA + Dunnett test.